Deletion of *Lrp4* increases the incidence of microphthalmia

Hiroshi Tanahashi[a*] and Tatsuo Suzuki[b]

[a]Department of Neuroplasticity, School of Medicine, Shinshu University, 3-1-1 Asahi, Matsumoto 390-8621, Japan, [b]Department of Molecular & Cellular Physiology, School of Medicine, Shinshu University, 3-1-1 Asahi, Matsumoto 390-8621, Japan

[*]Correspondence should be addressed to H.T. (E-mail: tanahashi_h@ybb.ne.jp)

Highlights

・The loss of *Lrp4* resulted in an elevated incidence of microphthalmia.

・The loss of *Lrp4* affected the mRNA expression of members of BMP, FGF, SHH and WNT signaling and of some microphthalmia genes for microphthalmia.

・The loss of *Lrp4* enhanced the incidence of the aberrant retinal folds, which appeared pleated and corrugated in the eyeball.

Abstract

Microphthalmia is a malformation that reduces the size of the ocular globe. The etiologies of this anomaly are various, but the genetic background appears to have a predominant influence on its development through mutations of genes controlling ocular developmental processes. LRP4 is a type I single transmembrane protein that is essential for the formation of neuromuscular junctions. We created and experimented on homozygous *Lrp4*-deficient mice and found the microphthalmia phenotype in their eyes. The loss of *Lrp4* resulted in an elevated incidence of microphthalmia and affected the mRNA expression of the members of bone morphogenetic protein, fibroblast growth factor, Sonic hedgehog, and WNT signaling pathways and of several pathogenic genes for microphthalmia. Moreover, the loss of *Lrp4* enhanced the incidence of aberrant retinal folds, which appeared pleated and corrugated in the eyeball.

Keywords

BMP; coloboma; fold; microphthalmia; SHH; WNT

Abbreviations

95% CI, 95% confidence interval; BMP, bone morphogenetic protein; FEVR, familial exudative vitreoretinopathy; FGF, fibroblast growth factor; LRP4; low-density lipoprotein receptor related protein 4; *Lrp4*$^{-/-}$, *Lrp4* homozygously null; *Lrp4*$^{+/-}$, *Lrp4* heterozygously null; MAC, microphthalmia, anophthalmia, and coloboma; OR, odds ratio; SHH, Sonic hedgehog

1. Introduction

Eye morphogenesis is a well-conserved process among vertebrates [1]. Many signaling pathways, including the bone morphogenetic protein (BMP), fibroblast growth factor (FGF), WNT, and Sonic hedgehog (SHH) pathways, control ocular developmental processes [2–4]. Developmental eye morphogenesis defects cause severe congenital eye malformations. Structural ocular anomalies, including microphthalmia (reduced ocular globe size), anophthalmia (ocular globe absence), and coloboma (optic fissure closure defects), have an estimated prevalence of 1 per 7,000, 1 per 30,000, and 1 per 5,000 live births, respectively [5–7]. To date, several mutations in genes that mediate ocular development and cause microphthalmia, anophthalmia, and coloboma (MAC) have been identified in humans and model animals [8, Supplementary Table S1].

LRP4 is a type I single transmembrane protein of the low-density lipoprotein receptor protein family. In muscles, LRP4 serves as a receptor for agrin and is essential for the activation of muscle-specific tyrosine kinase and the clustering of acetylcholine receptors, thus leading to the formation of neuromuscular junctions [9–11]. *Lrp4* knockout (*Lrp4*$^{-/-}$) mice have shown various aberrant phenotypes: a failure to develop neuromuscular junctions and dying of respiratory failure at birth [11,12], fully penetrant polysyndactyly [11–13], partially penetrant teeth abnormalities [13,14], impaired bone growth and increased bone turnover [15], delayed ureteric budding and partially penetrant kidney agenesis [11,12,16], small lung size [11,12], and amniotic fluid clearance pathways defects [12]. In addition, LRP4 can antagonize the canonical WNT signaling *in vitro* [13,17,18]. Here we further examined the functional role of LRP4 *in vivo* and found a novel phenotype of *Lrp4*$^{-/-}$ mice with partially penetrant eye abnormalities.

2. Materials and Methods

2.1. Mice

We generated *Lrp4*$^{+/-}$ heterozygotic mice [12] using the C57BL/6J congenic strain (B6 Thy1.1) derived embryonic stem cell line, Bruce4 [19], and then backcrossed with C57BL/6JJcl mice (CLEA Japan) for at least six generations. Homozygous *(Lrp4*$^{-/-}$) mice were obtained by intercrossing heterozygous (*Lrp4*$^{+/-}$) mice for 12 h starting at 9:00 in the evening. We denoted the day at which the vaginal plug was found at noon as E0.5. Genotyping was performed as described [12]. We measured eyeball right/left diameters using a digital FPC-BW08 microscope and the Micro-Measure software (Forever Plus Corp.). We conducted all animal experiments in strict accordance with the recommendations in the *Guidelines for Proper Conduct of Animal Experiments* (Science Council of Japan). The Committee on the Ethics of Animal Experiments of Shinshu University approved the protocol (Permit no. 270015). We carried out all surgeries under sevoflurane inhalation anesthesia (Mylan), and we made all efforts to minimize animal

suffering.

2.2. Tissue preparation for histological analyses

We prepared tissue sections by two methods: A and B. In Method A, we decapitated mouse embryos (E18.5) and fixed the cranial parts in Davidson's fixative (37.5% [v/v] methanol, 25% [v/v] formalin, and 12.5% [v/v] acetic acid) that has been reported to reduce artifacts (fixation-induced retinal folding [20]), for 24 h at 4°C. Next, we decalcified the samples in Morse's solution (10% [w/v] sodium citrate and 22% [v/v] formic acid) for 12 h at 4°C. Then, we cut the fixed cranial parts coronally near the eyeballs using a blade and then dehydrated the fixed specimens containing eyeballs through a graded series of alcohol, paraffin embedding, and coronal sections (3.75 μm) to obtain the best-aligned sections of the optic vesicle. We then processed the obtained sections for hematoxylin and eosin staining, or *in situ* hybridization (see below). In Method B, we used a double embedding technique to embed the tissues in accurate planes or to keep them in a proper orientation. We dissected the eyes out from formalin-fixed cranial parts. The specimens were superficially wrapped in 2% agarose (the first embedding), subjected to paraffin embedding (the second embedding), and then sectioned.

2.3. *In Situ* Hybridization

We amplified mouse *Lrp4* cDNA (NM_172668; nucleotide positions 6322–7094) by PCR and subcloned the PCR products into the pGEM-T Easy Vector (Promega). We set up *in vitro* transcriptions to synthesized digoxigenin-labeled antisense *Lrp4* RNA probes with the T7 RNA polymerase from *Sal* I -digested plasmid using the DIG RNA Labeling Kit (Roche). After hydrating the sections, we incubated them in an antigen retrieval solution HistoVT One (Nacalai Tesque) at 95°C for 40 min and washed them in TBS (Tris-buffered saline: 25 mM Tris [pH 7.4], 137 mM NaCl, and 2.68 mM KCl) thoroughly. We then subjected the sections to prehybridization in a hybridization buffer (50% formamide, 5x SSC [sodium chloride sodium citrate buffer], 5x Denhardt's solution, 0.25 mg/mL yeast tRNA, 0.5 mg/mL heat-denatured salmon sperm DNA) for 1 h at 23°C and then carried out hybridizations at 65°C for 18 h with a probe at a concentration of 1-2 μg/mL in a hybridization buffer. We performed three posthybridization washes in 0.2x SSC at 65°C for 20 min each. The sections were then blocked with 1.5% Blocking Reagent (Roche) at 24°C for 1 h and incubated at 24°C for 3 h with anti-digoxigenin-AP conjugate, Fab fragments (1: 500, Roche). After three washes in TBS every 20 min, we subjected the sections to colorimetric development in a BCIP (5-bromo-4-chloro-3-indolyl phosphate)–NBT (nitro blue tetrazolium) solution (Nacalai Tesque). We mounted the washed sections with covers on a slide and collected images using an Axio Observer Z1 light microscope (Zeiss).

2.4. RNA isolation and quantitative RT-PCR

We extracted total cellular RNA from the eyeballs using ISOGEN-II (Nippon Gene) according

to the manufacturer's instructions. cDNA was synthesized using ReverTra Ace® qPCR RT Master Mix with gDNA Remover (Toyobo) according to the manufacturer's instructions. Quantitative RT-PCR (qPCR) was set up using primers as described in Supplementary Table S1 and using THUNDERBIRD® SYBR qPCR Mix (Toyobo) on a StepOnePlus™ Real-Time PCR System (Thermo Fisher Scientific). All primers were first checked for their ability to specifically amplify defined mRNA regions. The signal values were normalized to *Gapdh* signals.

2.5. Statistical Analysis

Results are presented as means ± SD. For parametric test we tested data on the two groups for normality (F-test) and analyzed the significance using Student's *t*-test with or without Welch's correction. For nonparametric test we analyzed the significance, an odds ratio (OR) and corresponding 95% confidence internal (95% CI) using Fisher's exact test. In all the cases, we used the statistical software Prism 6.0 (GraphPad Software), and we considered differences to be statistically significant if $P < 0.05$.

3. Results

The qPCR analysis using fetal tissues at E18.5 revealed that *Lrp4* mRNA was expressed in all tissues that we examined, including in eyeballs, but most significantly in the lungs followed by the fetal membranes, with moderate expressions in the pancreas and olfactory bulbs (Fig. 1A). Our *in situ* hybridization analysis revealed that *Lrp4* mRNA was relatively highly expressed in the lens ectoderm (including the transitional zone), inner neuroblastic layer in the retina, ciliary marginal zone, ciliary muscle, and corneal epithelia in fetal eyeballs at E18.5 (Figs. 1B–1D). Thus, we concluded that *Lrp4* mRNA is expressed in the eyes.

Initially, we observed that the loss of *Lrp4* resulted in an elevated incidence of microphthalmia, as judged by gross examination [apparent small eye(s)] (Table 1 and Supplementary Table S2). Next, we measured the eyeball's right/left diameter, confirmed the normal distribution of data on the three groups, and defined microphthalmia as an eyeball with a at least two SDs below the mean (inferior extremity of 95% CI) for mice in the same developmental stage (Table 1 and Supplementary Table S2). The incidence of microphthalmia in $Lrp4^{-/-}$ mice was higher than that in their wild-type and $Lrp4^{+/-}$ littermates as well. Right eyes were more often affected than the left ones, and when both were affected, there was a tendency for the right one to be more severely affected than the other one (Table 1 and Supplementary Table S2). Similar findings (affected right sides predominated) have been reported for newborn inbred C57BL/6JKt mice [21] and *Dkk1* (an antagonist of the canonical Wnt signaling) heterozygous null mice [22]. Microphthalmia in $Lrp4^{-/-}$ mice showed variations in deformity. About 48% of $Lrp4^{-/-}$ mice with microphthalmia had accompanying ocular coloboma (Table 1). We observed

microphthalmia associated with typical ocular coloboma and a small pupil in *Lrp4*$^{-/-}$ mice (Figs. 2A, 2B and Supplementary Fig. S1). One eye in an *Lrp4*$^{-/-}$ mouse was visible through the fused eyelids (Fig. 2C), whereas the other eye was not visible externally (Fig. 2D). Dissection of this mutant head revealed a very small eye with a little abnormal retinal tissue, but buried within the skull, directly beneath the brain (Fig. 2F).

The morphology of the retinas in *Lrp4*$^{-/-}$ mice was examined by histochemical analysis, and we confirmed the failure of the optic fissure closure in *Lrp4*$^{-/-}$ fetal eye (Fig. 3A–C). In addition, in some *Lrp4*$^{-/-}$ and control (wild-type and *Lrp4*$^{+/-}$) mice, the inner neuroblastic layer of the retina appeared to have an aberrant form, and a portion of the retina (Fig. 3D, E, K, and M) or a nodule of dysplastic primary vitreous (Fig. 3F, N, O, and P) was attached to the posterior lens. Eight out of 32 *Lrp4*$^{-/-}$ mice had aberrant retinal folds, which appeared pleated and corrugated in the eyeball (Table 2 and Fig. 3H–P). On the other hand, three out of 48 control mice carried retinal folds (Table 2 and Fig. 3D–G). The right retinas were more often affected than the left ones, and microphthalmia enhanced the incidence of retinal folds in both *Lrp4*$^{-/-}$ and control mice (Table 2). Five (Fig. 3H–M) out of the 26 *Lrp4*$^{-/-}$ mice without microphthalmia presented retinal folds, whereas only one (Fig. 3D, and E) out of 42 control mice without microphthalmia presented retinal folds. Thus, the loss of *Lrp4* enhanced the incidence of the retinal folds (OR: 9.76, 95% CI: 1.07-89.1 [*Lrp4*$^{-/-}$ vs wild-type + *Lrp4*$^{+/-}$], $P < 0.05$).

To understand the molecular mechanisms of the aberrant ocular phenotypes of *Lrp4*$^{-/-}$ mice, we performed qPCR analyses of the eyeballs isolated from E18.5 using specific primers for 69 genes related to MAC and eye development, including BMP, SHH, FGF, and WNT signaling (Supplementary Table S1). Twenty mRNAs for *Foxe3*, *Pax6*, *Pitx3*, *Shh*, *Wnt7α*, *Bmp2*, *Bmp4*, *Bmp7*, *Smad1*, *Id1*, *Id2*, *Id3*, *Ptch1*, *Smo*, *Gli1*, *Gli2*, *Gli3*, *Fgfr1*, *Fgfr3*, and *Yap1* genes were downregulated in *Lrp4*$^{-/-}$ eyes compared to those in the wild-type eyes (Table 3). The mutants of seven genes—*Foxe3*, *Pax6*, *Pitx3*, *Shh*, *Bmp4*, *Bmp7*, and *Yap1*—have been shown to generate MAC phenotypes (Table 3).

4. Discussion

In the present report, we described a novel microphthalmia phenotype of *Lrp4*$^{-/-}$ mice and presented the possible causes for it. BMP4 and BMP7 are implicated in the control of multiple events during eye development in mice. BMP4 heterozygous null mice [23] and BMP7 knockout mice [27,28] have shown either anophthalmia or microphthalmia (35% in [23], 96% in [24], and 71% in [25]). ID1, ID2, and ID3 are targets of BMP signaling for the differentiation of retinal progenitor cells [26], and the mRNA expressions were reduced in *Lrp4*$^{-/-}$ mice (Table 2). Inactivation of the downstream effector of BMPs, SMAD4, in the ocular surface ectoderm that forms the lens, cornea, and eyelids leads to microphthalmia and retinal dysplasia and affects

the expression of members of BMP, SHH, and WNT signaling pathways in the retina [27], including the *Bmp7*, *Gli2*, *Gli3*, *Ptch1*, and *Smo* mRNAs whose expressions were reduced in our *Lrp4*$^{-/-}$ mice at E18.5 (Fig. 3). In addition, disruption of *Lrp4* decreased the expression of the *Foxe3* and *Pitx3* mRNAs that were also reduced in E10.5 embryo eyes with conditionally deleted *Bmp4* from the optic vesicle [28]. These results suggest that the loss of *Lrp4* affects the expression of members of BMP and SHH signaling pathways, resulting in microphthalmia. Similarly, studies have reported that the deletion of *Lrp4* leads to expression pattern changes including ectopic expression of some molecules involving WNT, BMP, FGF, and SHH signaling in the apical ectodermal ridge (*Wnt7α*, *Bmp2*, *Bmp4*, *Fgf8*, *Shh*, and *Gli1* mRNA), in developing teeth (*Bmp4*, *Bmp7*, *Shh*, *Gli2*, and *Ptch1* mRNA), and in developing kidneys (*Wnt11* mRNA) [13,14,16].

Histochemical analysis of all *Lrp4*$^{-/-}$ mice with aberrant retinal folds revealed retention of both lenses. In contrast, in ocular surface ectoderm-specific *Smad4* knockout mice with aphakia, the retina appeared pleated and corrugated, whereas in the mutants with microphthalmia (but not aphakia), the retina formed a proper cup-like structure [27]. *Lrp4* conventional knockout mice may be susceptible to retinal folds. In humans, such retinal folds are seen in Norrie's disease [29] or in patients with familial exudative vitreoretinopathy (FEVR) [30]. Mutations in the *NDP* gene cause Norrie's disease, and mutations in the *FZD4*, *LRP5*, or *NDP* gene cause FEVR. These gene products are WNT signaling transmission proteins that participate in the development of the retinal vasculature. Pathogenic mutations cause defective retinal angiogenesis, resulting in retinal ischemia, retinal folds, and retinal detachments. Although further studies are needed for confirmation, our study suggests that the loss of the WNT-modulator LRP4 participates in aberrant retinal fold.

Author Contributions

H.T. conceived, designed and performed experiments, interpreted data, and wrote the manuscript. All authors reviewed the manuscript.

Acknowledgments

We thank Ms. Misako Yamada and Ms. Kayo Suzuki (Shinshu University) for helping hematoxylin and eosin staining. We also thank Professor Naoto Saito (Shinshu University) for his hospitality. This research did not receive any specific grant from funding agencies in the public, commercial, or not-for-profit sectors.

References

[1] J. Graw, Eye development, Curr. Top. Dev. Biol. 90 (2010) 343-386.

[2] S. Bassnett, H. Sikic, The lenz growth process, Prog. Retin. Eye Res. 60 (2017) 181-200.

[3] L. Gunhaga, The lens: a classical model of embryomic induction providing new insights into cell determination in early development, Phil. Trans. R. Soc. B, 366 (2011) 1193-1203.

[4] S. Fuhrmann, Eye morphogenesis and patterning of the optic vesicle, Curr. Top. Dev. Biol. 93 (2010) 61-84.

[5] D. Morrison, D. FitzPatrick, I. Hanson, et al., National study of microphthalmia, anophthalmia, and coloboma (MAC) in Scotland: investigation of genetic aetiology, J. Med. Genet. 39 (2002) 16-22.

[6] S.P. Shah, A.E. Taylor, J.C. Sowden, et al., Anophthalmos, microphthalmos, and typical coloboma in the United Kingdom: a prospective study of incidence and risk, Invest. Ophthalmol. Vis. Sci. 52 (2011) 558-564.

[7] A.S. Verma, D.R. Fitzpatrick, Anophthalmia and microphthalmia, Orphanet. J. Rare Dis. 2 (2007) e47.

[8] K.A. Williamson, D.R. Fitzpatrick, The genetic architecture of microphthalmia, anophthalmia and coloboma, Eur. J. Med. Genet. 57 (2014) 369-380.

[9] B. Zhang, S. Luo, Q. Wang, et al., LRP4 serves as a coreceptor of agrin, Neuron 60 (2008) 285-297.

[10] N. Kim, A.L. Stiegler, T.O. Cameron, et al., Lrp4 is a receptor for Agrin and forms a complex with MuSK, Cell 135 (2008) 334-342.

[11] S.D. Weatherbee, K.V. Anderson, L.A. Niswander, LDL-receptor-related protein 4 is crucial for formation of the neuromuscular junction, Development 133 (2006) 4993-5000.

[12] H. Tanahashi, Q.B. Tian, Y. Hara, et al., Polyhydramnios in *Lrp4* knockout mice with bilateral kidney agenesis: Defects in the pathways of amniotic fluid clearance, Sci. Rep. 6 (2016) e20241.

[13] E.B. Johnson, R.E. Hammer, J. Herz, Abnormal development of the apical ectodermal ridge and polysyndactyly in Megf7-deficient mice, Hum. Mol. Genet. 14 (2005) 3523-3538.

[14] A. Ohazama, E.B. Johnson, M.S. Ota, et al., Lrp4 modulates extracellular integration of cell signaling pathways in development, PLoS One 3 (2008) e4092.

[15] H.T. Choi, M. Dieckmann, J. Herz, et al., Lrp4, a novel receptor for Dickkopf 1 and sclerostin, is expressed by osteoblasts and regulates bone growth and turnover in vivo, PLoS One 4 (2009) e7930.

[16] C.M. Karner, M.F. Dietrich, E.B. Johnson, et al., Lrp4 regulates initiation of ureteric budding and is crucial for kidney formation-a mouse model for Cenani-Lenz syndrome, PLoS One 5 (2010) e10418.

[17] Y. Li, B. Pawlik, N. Elcioglu, et al., LRP4 mutations alter Wnt/beta-catenin signaling and cause limb and kidney malformations in Cenani-Lenz syndrome, Am. J. Hum. Genet. 86 (2010) 696-706.
[18] M.F. Dietrich, L. van der Weyden, H.M. Prosser, et al., Ectodomains of the LDL receptor-related proteins LRP1b and LRP4 have anchorage independent functions in vivo, PLoS One 5 (2010) e9960.
[19] F. Kontgen, G. Suss, C. Stewart, et al., Targeted disruption of the MHC class Ⅱ Aa gene in C57BL/6 mice, Int. Immunol. 5 (1993) 957-964.
[20] J. Frencha, J. Hallidayb, M. Scottb, et al., Retinal folding in the term rabbit fetus—Developmental abnormality or fixation artifact? Reproductive Toxicology 26 (2008) 262–266.
[21] H. Kalter, Sporadic congenital malformations of newborn inbred mice, Teratology 1 (1968) 193-200.
[22] O. Lieven, U. Rüther, The Dkk1 dose is critical for eye development, Dev. Biol. 355 (2011) 124–137.
[23] N.R. Dunn, G.E. Winnier, L.K. Hargett, et al., Haploinsufficient phenotypes in *Bmp4* heterozygous nullmice and modification by mutations in *Gli3* and *Alx*, Dev. Biol. 188 (1997) 235-247.
[24] A.T. Dudley, K.M. Lyons, E.J. Robertson, A requirement for bone morphogenetic protein-7 during development of the mammalian kidney and eye, Genes & Dev. 9 (1995) 2795-2807.
[25] G. Luo, C. Hofmann, A.L. Bronckers, et al., BMP-7 is an inducer of nephrogenesis, and is also required for eye development and skeletal patterning, Genes & Dev. 9 (1995) 2808-2820.
[26] Y. Du, Q. Xiao, H.K. Yip, Regulation of retinal progenitor cell differentiation by bone morphogenetic protein 4 is mediated by the Smad/Id cascade, Invest. Ophthalmol. Vis. Sci. 51 (2010) 3764-3773.
[27] J. Li, S. Wang, C. Anderson, et al., Requirement of Smad4 from ocular surface ectoderm for retinal development, PLoS One 11 (2016) e0159639.
[28] J. Huang, Y. Liu, A. Oltean, et al., Bmp4 from the optic vesicle specifies murine retinal formation, Dev. Biol. 402 (2015) 119-126.
[29] M. Michaelides, P.J. Luthert, R. Cooling, et al., Norrie disease and peripheral venous insufficiency, Br. J. Ophthalmol. 88 (2004) 1475.
[30] M. Nishimura, T. Yamana, M. Sugino, et al., Falciform retinal fold as sign of familial exudative vitreoretinopathy, Jpn. J. Ophthalmol. 27 (1983) 40–53.
[31] L.A. Schimmenti, J. de la Cruz, R.A. Lewis, Novel mutation in Sonic hedgehog in non-syndromic colobomatous microphthalmia, Am. J. Med. Genet. 116A (2003) 215-221.
[32] P. Bakrania, S.A. Ugur Iseri, A.W. Wyatt, et al., Sonic hedgehog mutations are an

uncommon cause of developmental eye anomalies, Am. J. Med. Genet. 152A (2010) 1310-1313.
[33] A. Alldredge, S. Fuhrmann, Loss of Axin2 Causes Ocular Defects During Mouse Eye Development, Invest. Ophthalmol. Vis. Sci. 57 (2016) 5253-5262.
[34] D. Becker, J. Tetens, A. Brunner, et al., Microphthalmia in Texel sheep is associated with a missense mutation in the paired-like homeodomain 3 (PITX3) gene, PLoS One 5 (2010) e8689.

Legends to figures

Fig. 1 | *Lrp4* expression in mouse E18.5 fetus (A) Real-time qPCR analysis of *Lrp4* expression in various tissue RNAs from E18.5 fetuses. For all experiments, two biological replicates were analyzed. The mean of cerebrum was set as 1, and each value of the tissues was a relative ratio to the mean of cerebrum. (B-D) *In situ* hybridization analysis of *Lrp4* expression in $Lrp4^{-/-}$ fetal eye (B) and wild-type littermate (C) at E18.5. (D) magnification of a square in (C). *Lrp4* mRNA was relatively highly expressed in the lens ectoderm (including the transitional zone) (le), inner neuroblastic layer in retina (in), ciliary marginal zone (cmz), ciliary muscle (cm), and corneal epithelia (ce).

Fig. 2 | Microphthalmia and ocular coloboma in E18.5 $Lrp4^{-/-}$ fetus (A, E) Skin was removed from the fetal cranial part. (B) Microphthalmia with ocular coloboma and a small pupil in a right eye was observed. (C, D) A right eye in an $Lrp4^{-/-}$ fetus was visible through the fused eyelids (C), whereas a left eye was not visible externally (D). (F) Dissection of this mutant head revealed a very small eye with a little abnormal retinal tissue, but buried within the skull, directly beneath the brain.

Fig. 3 | Morphology of aberrant retina phenotypes We used both samples from wild-type and $Lrp4^{+/-}$ mice as controls (Ctrl), because they were phenotypically indistinguishable. (A–C) Failure of the optic fissure closure in E14.5 $Lrp4^{-/-}$ fetal eye. (B) Coronal section of optic fissure at midlenticular levels. (C) Magnification of a square in (B). (D–F, K, M–P) A portion of the retina (D, E, K, M) or a nodule of dysplastic primary vitreous (F, N–P) was attached to the posterior lens. (D–P) Pleated and corrugated retina (retinal folds). (D and E, H and I) Left and right eyes derived from the same mouse. KO: $Lrp4^{-/-}$ mouse, Ctrl: wild-type or $Lrp4^{+/-}$ mouse. Scale bars: B, D–P, 500 μm; C,100 μm.

Fig.1

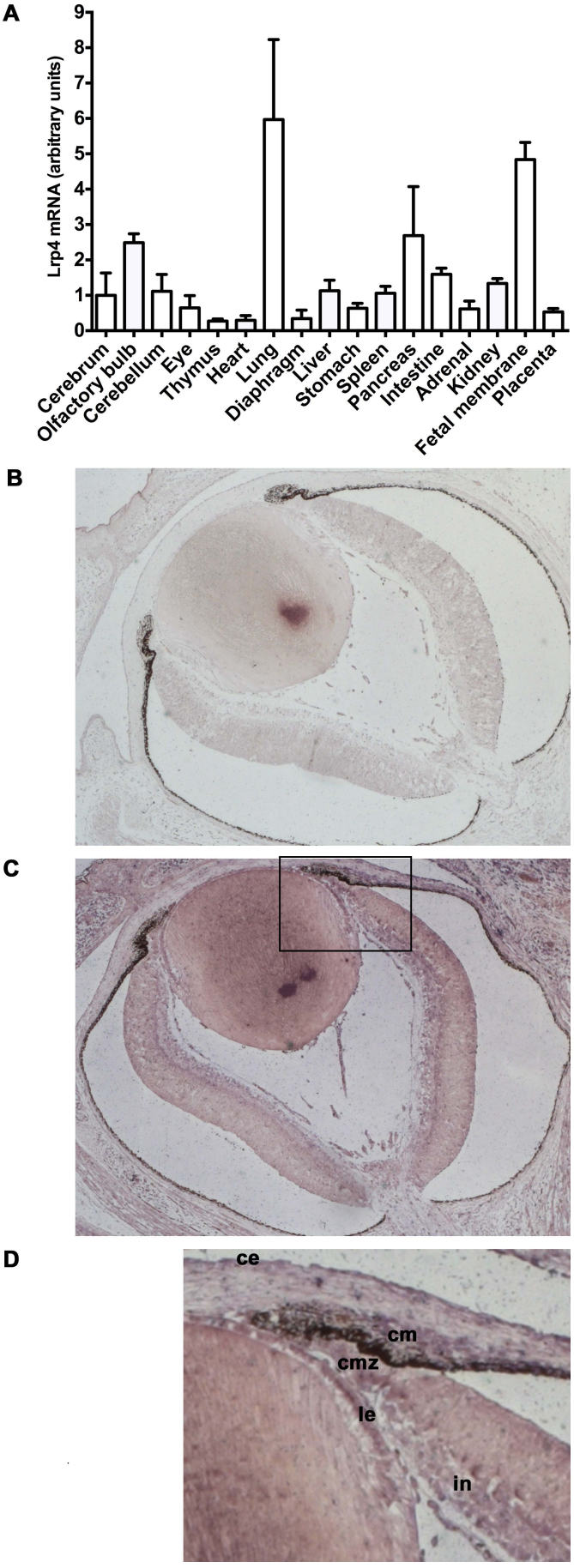
A
Lrp4 mRNA (arbitrary units)
0
1
2
3
4
5
6
7
8
9
Cerebrum
Olfactory bulb
Cerebellum
Eye
Thymus
Heart
Lung
Diaphragm
Liver
Stomach
Spleen
Pancreas
Intestine
Adrenal
Kidney
Fetal membrane
Placenta
B
C
D
ce
cm
cmz
le
in

Fig.2

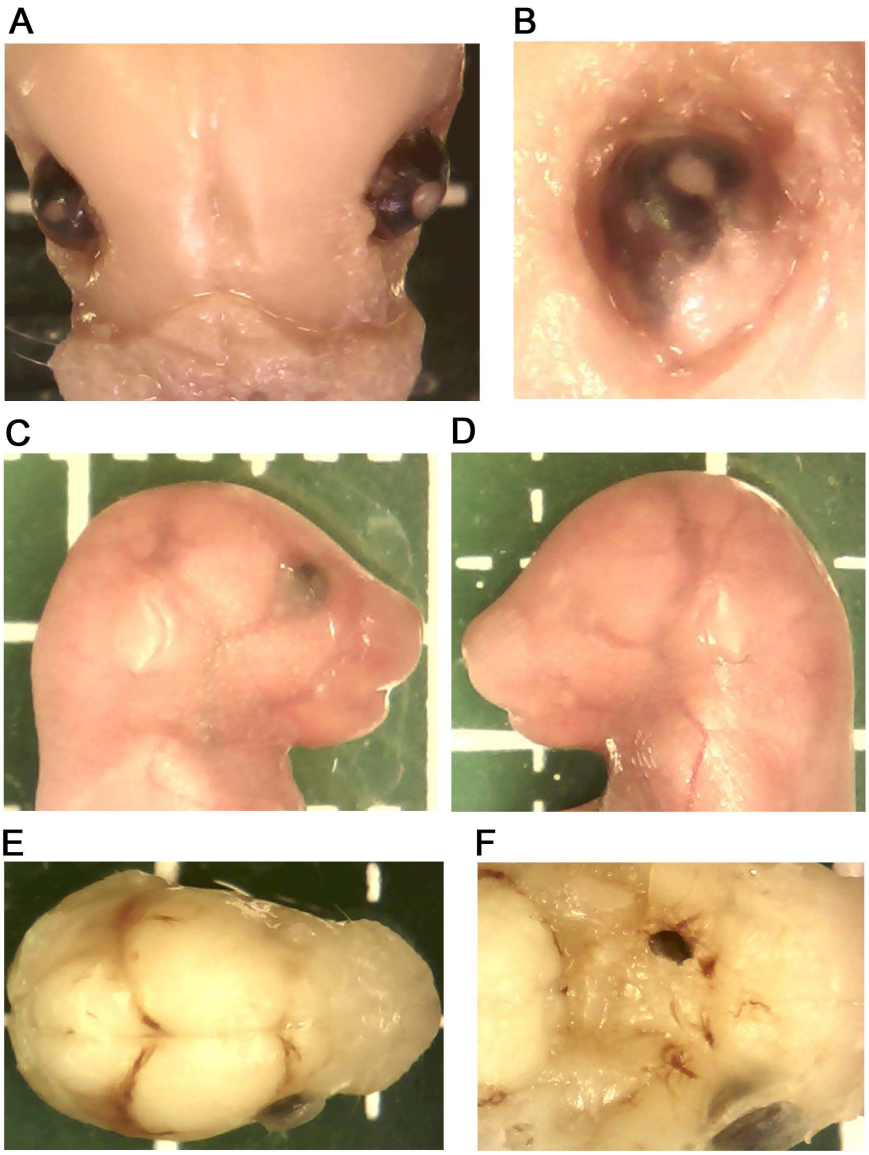

Fig.3

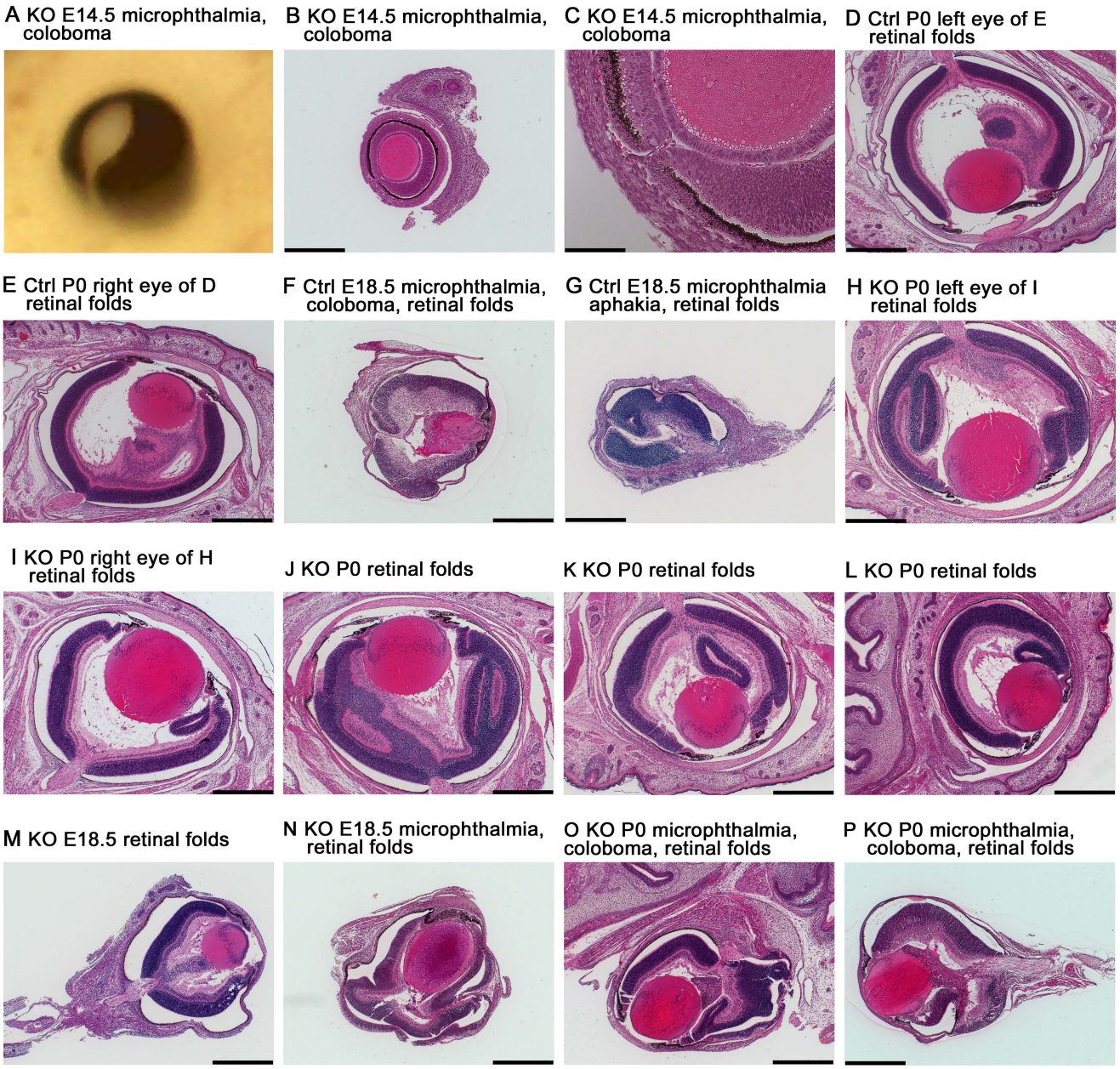
A KO E14.5 microphthalmia, coloboma
B KO E14.5 microphthalmia, coloboma
C KO E14.5 microphthalmia, coloboma
D Ctrl P0 left eye of E retinal folds
E Ctrl P0 right eye of D retinal folds
F Ctrl E18.5 microphthalmia, coloboma, retinal folds
G Ctrl E18.5 microphthalmia aphakia, retinal folds
H KO P0 left eye of I retinal folds
I KO P0 right eye of H retinal folds
J KO P0 retinal folds
K KO P0 retinal folds
L KO P0 retinal folds
M KO E18.5 retinal folds
N KO E18.5 microphthalmia, retinal folds
O KO P0 microphthalmia, coloboma, retinal folds
P KO P0 microphthalmia, coloboma, retinal folds

Table 1 | Incidence of mice with microphthalmia and coloboma

genotype	microphthalmia	coloboma	microphthalmia with coloboma
Mice with microphthalmia judged by gross examination			
wild-type	5 (4 right; 1 both[*1]) / 378 (1.3%)	2 (2 right) / 378	2 (2 right) / 378
Lrp4$^{+/-}$	7 (2 left; 5 right) / 672 (1.0%)	5 (1 left; 4 right) / 672	2 (2 right) / 672
Lrp4$^{-/-}$	28[#1] (5 left; 21 right; 2 both[*2]) / 304 (9.2%)	14[#1] (3 left; 11 right) / 304	11[#1] (2 left; 9 right) / 304
	[#2]OR=8.78 (4.40-17.5)	[#2]OR=7.23 (2.89-18.1)	[#2]OR=9.82 (3.10-31.1)
Mice with microphthalmia defined as an eyeball with a at least two SDs below the mean of left/right diameter			
wild-type	3 (2 right; 1 both) / 187 (1.6%)	2 (2 right) / 187	1 (1 right) / 187
Lrp4$^{+/-}$	5 (1 left; 3 right; 1 both) / 357 (1.4%)	5 (1 left; 3 right; 1 both) / 357	4 (3 right; 1 both) / 357
Lrp4$^{-/-}$	20[#1] (4 left; 14 right; 2 both[*2]) / 174 (11.5%)	14[#1] (2 left; 12 right) / 174	12[#1] (2 left; 10 right) / 174
	[#2]OR=8.70 (3.76-20.1)	[#2]OR=6.71 (2.66-16.9)	[#2]OR=7.99 (2.77-23.0)

In all, fetuses at E14.5 (177 fetuses), E16.5 (229 fetuses) and E18.5 (917 fetuses), and 749 newborns (P0) were examined. Details are described in Supplementary Table S2. [*1]Otocephaly with microphthalmia on both eyes. [*2]Right eye had accompanying coloboma. [#1]*P*-value of statistics < 0.0001 (*Lrp4*$^{-/-}$ vs wild-type + *Lrp4*$^{+/-}$). [#2]OR for dominance with respect to *Lrp4*$^{-/-}$ and corresponding 95% CI (*Lrp4*$^{-/-}$ vs wild-type + *Lrp4*$^{+/-}$). Microphthalmia and coloboma were more frequently identified on the right side of *Lrp4*$^{-/-}$ mice (microphthalmia 39 right and 13 left; OR: 3.00, 95% CI: 1.31-6.88, coloboma 23 right and 5 left; OR: 4.60, 95% CI: 1.36–15.6). This was significantly different from the expected proportion.

Table 2 | Summary of aberrant retina phenotypes (Fig. 3) in histochemically examined mice.

genotype (number)	mice with microphthalmia	mice with retinal folds	mice with retina attached to the posterior lens	mice with dysplastic primary vitreous
wild-type & *Lrp4*$^{+/-}$ (48)	6[*1](6 right)	3[*1](2 right; 1both; 2 microphthalmia)	1 (1 both)	1 (1 right; 1 microphthalmia)
Lrp4$^{-/-}$ (32)	6 (2 left; 4 right)	8 (2 left; 5 right; 1both; 3 microphthalmia)	2 (1 left; 1 right)	3 (3 right; 3 microphthalmia)

In all, fetuses at E14.5 (1 *Lrp4*$^{-/-}$), E16.5 (1 *Lrp4*$^{+/-}$) and E18.5 (17 wild-type & *Lrp4*$^{+/-}$; 9 *Lrp4*$^{-/-}$), and P0 [30 wild-type & *Lrp4*$^{+/-}$; 22 *Lrp4*$^{-/-}$] were examined.[*1]One mouse also presented aphakia on the right eye.

Table 3 | Differentially expressed genes in wild-type and *Lrp4*$^{-/-}$ fetal eyeballs at E18.5

Genes	Fold mRNA change *Lrp4*$^{-/-}$ mice / wild-type mice ±SD	Protein function: existence of reports of MAC phenotypes in the mutants (reference number).
BMP signaling		
Bmp2	0.686±0.337	Secreted signaling molecule in the BMP family protein: No
Bmp4	0.638±0.256	Secreted signaling molecule in the BMP family protein, regulated by WNT signaling in colon cancer cells: Yes (8)
Bmp7	0.649±0.362	Secreted signaling molecule in the BMP family protein: Yes (8)
Smad1	0.675±0.271	Downstream effector of BMPs: No
Id1	0.743±0.210	Gene regulated by BMP-Smad signaling in retinal ganglion cells: No
Id2	0.753±0.200	Gene regulated by BMP-Smad signaling in retinal ganglion cells: No
Id3	0.711±0.250	Gene regulated by BMP-Smad signaling in retinal ganglion cells: No
SHH signaling		
Shh	0.463±0.228	Secreted signaling molecule of hedgehog protein family: Yes (31,32)
Ptch1	0.691±0.458	Membrane receptor for SHH and SMO, SHH-PTCH1 releases SMO and induces SMO activity: No
Smo	0.644±0.250	Downstream effector of SHH signaling: No
Gli1	0.698±0.408	Downstream effector of SHH signaling: No
Gli2	0.621±0.329	Downstream effector of SHH signaling: No
Gli3	0.726±0.388	Downstream effector of SHH signaling: No
FGF signaling		
Fgfr1	0.630±0.321	Membrane receptor for FGFs ligands: No
Fgfr3	0.759±0.316	Membrane receptor for FGFs ligands: No
WNT signaling		
Wnt7α	0.463±0. 338	Secreted signaling molecule in the WNT family protein: No.
Other gene related to MAC		
Foxe3	0.561±0.415	Forkhead transcription factor: Yes (33)
Pax6	0.730±0.313	Paired box transcription factor: Yes (8)
Pitx3	0.677±0.431	Paired-like homeodomain transcription factor: Yes (34)
Yap1	0.589±0.256	Hipp pathway effector: Yes (8)

Real-time qPCR analyses of 69 genes related to MAC and eye development, including BMP, SHH, FGF and WNT signaling were performed (Supplemental Table S1). Twenty-nine wild-type and 19 *Lrp4*$^{-/-}$ fetal eyeballs at E18.5 were analyzed. Differentially expressed genes (P<0.05) in wild-type and *Lrp4*$^{-/-}$ eyeballs are shown.

Deletion of *Lrp4* increases the incidence of microphthalmia

Hiroshi Tanahashi[a*] and Tatsuo Suzuki[b]

[a]Department of Neuroplasticity, School of Medicine, Shinshu University, 3-1-1 Asahi, Matsumoto 390-8621, Japan, [b]Department of Molecular & Cellular Physiology, School of Medicine, Shinshu University, 3-1-1 Asahi, Matsumoto 390-8621, Japan

[*]Correspondence should be addressed to H.T. (E-mail: tanahashi_h@ybb.ne.jp)

Supplementary Data

Supplementary Fig. S1 | Microphthalmia with coloboma in E18.5 *Lrp4*$^{-/-}$ fetuses (A, D) Front faces. (B, E) Skin was removed from the cranial part of A and D. (C, F) Eyes were dissected out from B and E. Microphthalmia with coloboma was observed on the right eye.

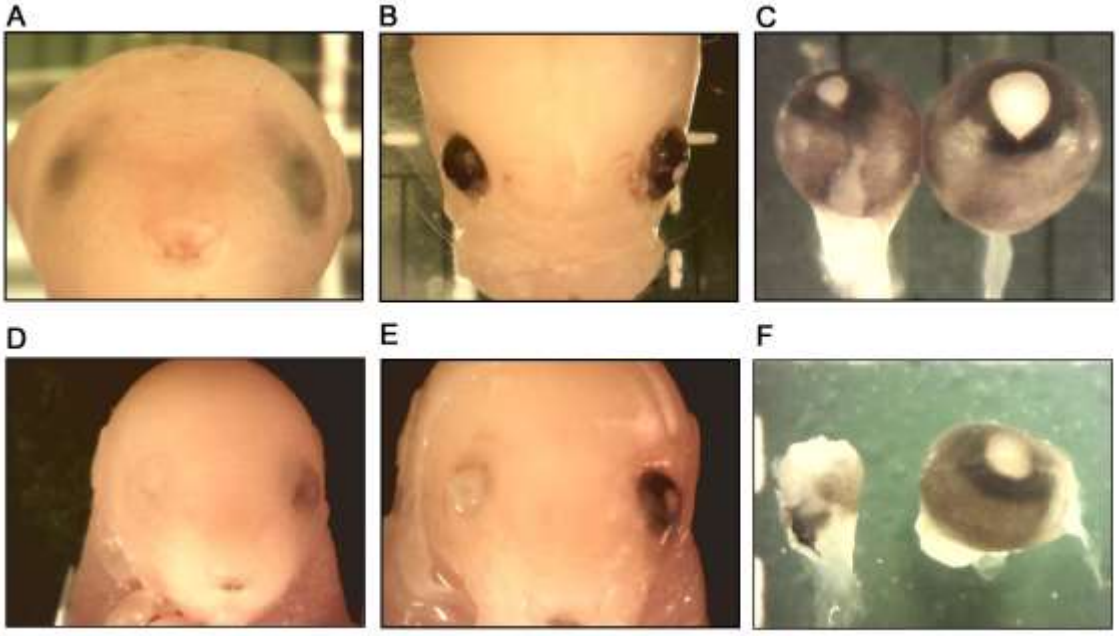

Supplementary Table S1 | Analyzed genes and oligonucleotide primers used for qPCR.

WNT signaling pathway	Protein function: existence of reports of MAC*[1] phenotypes in the mutants (reference number).
Wnt2bF 5'-CCGAGGTGGCAAACATCCTA-3' Wnt2bR 5'-TCGTGGAACGTGCAGTAGTT-3'	Secreted signaling molecule in the WNT family protein: No
Wnt4F 5'-TCTCTGCTCATTGTCCAT-3' Wnt4R 5'-TGCTGAACTAAGTCTACCA-3'	Secreted signaling molecule in the WNT family protein: No
Wnt5aF 5'-ACAGGCATCAAGGAATGCCA-3' Wnt5aR 5'-CGGCTGCCTATTTGCATCAC-3'	Secreted signaling molecule in the WNT family protein: No
Wnt7aF 5'-ATAGTCTACCTCCGGATCGGTG-3' Wnt7aR 5'-CTCCCGACTCCCCACTTTGAG-3'	Secreted signaling molecule in the WNT family protein: No
Wnt7bF 5'-GCCAATCTTCCATTCCATT-3' Wnt7bR 5'-CCTCTGTCCATCTGTCAT-3'	Secreted signaling molecule in the WNT family protein: No
Wnt9bF 5'-CTTGAAGTTGAGGCTGAG-3' Wnt9bR 5'-ATGTATGAGGTAGGCAGAA-3'	Secreted signaling molecule in the WNT family protein: No
Fzd5F 5'-GTGCTTCATCTCCACGTCCA-3' Fzd5R 5'-CAGGTAGCACGCAGACAAGA-3'	Membrane receptor for WNT ligands: Yes (S1)
Fzd7F 5'-ACCCTACTGCTCCCTACCTG-3' Fzd7R 5'-AGAAGGGGAAAGACAAGCGG-3'	Membrane receptor for WNT ligands: No
Axin2F 5'-ACAGCATCTTCACCACTTTG-3' Axin2R 5'-AGAAACCCTCACTTCCTAAAGAG-3'	Regulator of the stability of beta-catenin gene regulated by WNT-signaling: Yes (S2)
Lef1F 5'-GAACACCCTGATGAAGGAAAGC-3' Lef1R 5'-CACGGGCACTTTATTTGATGTC-3'	WNT effector transcription factor, gene regulated by WNT-signaling in colon cancer: No.
Tcf4F 5'-AGCCCGTCCAGGAACTATG-3' Tcf4R 5'-TGGAATTGACAAAAGGTGGA-3'	WNT effector transcription factor: No
MycF 5'-ACCACCAGCAGCGACTCTGAAG-3' MycR 5'-TGGCACCTCTTGAGGACCAGTG-3'	Gene regulated by WNT signaling: No
Twist2F 5'- CTGCTCAGCTAGCCGTGTTT-3' Twist2R 5'-TCCTGGGTGTGGAGCGTTAT-3'	Gene regulated by WNT signaling: No
BMP Smad signaling pathway	Protein function: existence of reports of MAC*[1] phenotypes in the mutants (reference number).
Bmp2F 5'-ACCCCCAGCAAGGACGTCGT-3' Bmp2R 5'-AAGAAGCGCCGGGCCGTTTT-3'	Secreted signaling molecule in the BMP family protein: No
Bmp3F 5'-AGCAGTGGGTCGAACCTCGGA-3' Bmp3R 5'-ACCCCCACCGCTCGCACTAT-3'	Secreted signaling molecule in the BMP family protein: No

BMP Smad signaling pathway	Protein function, existence of reports of MAC*[1] phenotypes in the mutants (reference number).
Bmp3bF 5'-GGCAACACCGTCCGAAGCTTCC-3' Bmp3bR 5'-AGGAGGCGGCAGGATGCGTT-3'	Secreted signaling molecule in the BMP family protein: No
Bmp4F2 5'-CGAGCCAACACTGTGAGGAGTTTC-3' Bmp4R2 5'-TTCTCTGGGATGCTGCTGAGGTT-3'	Secreted signaling molecule in the BMP family protein, regulated by WNT signaling in colon cancer cells: Yes (S3)
Bmp5F 5'-ATCAGGACCCCTCCAGGATGCC-3' Bmp5R 5'-TGATCCAGTCCTGCCATCCCAGATC-3'	Secreted signaling molecule in the BMP family protein: No
Bmp6F 5'-GCAGAGTCGCAACCGGTCCA-3' Bmp6R 5'-GGTGCAATGATCCAGTCCTGCC-3'	Secreted signaling molecule in the BMP family protein: No
Bmp7F 5'-CAAGCAGCGCAGCCAGAATCG-3' Bmp7R 5'-CAATGATCCAGTCCTGCCAGCCAA-3'	Secreted signaling molecule in the BMP family protein: Yes (S3)
Bmp8aF 5'-TTGGCTGGCTGGACTGGGTCA-3' Bmp8aR 5'-GCTGTCATAGTACAGCACAGAGGTG-3'	Secreted signaling molecule in the BMP family protein: No
Bmp8bF 5'-GGCTGGCTGGACTCTGTCATTGC-3' Bmp8bR 5'-AGCTCAGTAGGCACACAGCACAC-3'	Secreted signaling molecule in the BMP family protein: No
Bmp10F 5'-GACTCCTGGATCATCGCTCCTC-3' Bmp10R 5'-CAAGGCCTGAATAATTGCGTGTT-3'	Secreted signaling molecule in the BMP family protein: No
Bmp15F 5'-GCCGTCGGCCAACACAGTAAG-3' Bmp15R 5'-AGAAGGTAAGTGCTTGGTCCGGCA-3'	Secreted signaling molecule in the BMP family protein: No
Bmpr1aF 5'-GGTCAAAGCTGTTCGGAGA-3' Bmpr1aR 5'-CTGTACACGGCCCTTTGAAT-3'	Membrane receptor for BMPs ligands: No
Bmpr1bF 5'-TCAATGTCGTGACACTCCCATTCCT-3' Bmpr1bR 5'-TGCTGTACCGAGGTCGGGCT-3'	Membrane receptor for BMPs ligands: No
Bmpr2F 5'-CACCCCCTGACACAACACCACTC-3' Bmpr2R 5'-GACCCCGTCCAATCAGCTCCAG-3'	Membrane receptor for BMPs ligands: No
Smad1F 5'-GTTCAGGCAGTTGCTTACGA-3' Smad1R 5'-ATTGTTGGACGGATCTGTGA-3'	Downstream effector of BMPs: No
Smad4F 5'-AGGTGGCCTGATCTACACAAG-3' Smad4R 5'-ACCCGCTCATAGTGATATGGATT-3'	Downstream effector of BMPs: Yes (S4,S5)
Smad5F 5'-GGCAGTGGATGCTTTAGTGA-3' Smad5R 5'-GAGAAACTTGCAGACGTCCA-3'	Downstream effector of BMPs: No
Smad8/9F 5'-CAGCCTCAAGGTCTTCAACA-3' Smad8/9R 5'-CTTCACAAAGCTCATCCGAA-3'	Downstream effector of BMPs: No
Id1F 5'-ACATGAACGGCTGCTACTCACG-3' Id1R 5'-CGACTTCAGACTCCGAGTTCAG-3'	Gene regulated by BMP-Smad signaling in retinal ganglion cells: No

Id2F 5’-TCCAAGCTCAAGGAACTGG-3’ Id2R 5’-ATTCAGATGCCTGCAAGGAC-3’	Gene regulated by BMP-Smad signaling in retinal ganglion cells: No
Id3F 5’-AGGTGTCTCTTTTCCTCCCT-3’ Id3R 5’-ATGTCGTCCAAGAGGCTAAG-3’	Gene regulated by BMP-Smad signaling in retinal ganglion cells: No
SHH signaling pathway	Protein function: the existence of reports of MAC*[1]phenotypes in the mutants (reference number).
ShhF 5’-ACCTTCAAGAGCCTTAACT-3’ ShhR 5’-GCATAGCAGGAGAGGAAT-3’	Secreted signaling molecule of hedgehog protein family: Yes (S6,S7)
Ptch1F 5’-CTGCCTGTCCTCTTATCC-3’ Ptch1R 5’-CTGCTGTGCTTCGTATTG-3’	Membrane receptor for SHH and SMO. SHH-PTCH1 releases SMO and induces SMO activity: No
Ptch2F 5’-ACAAGCTGCTCATCCAAACC-3’ Ptch2R 5’-TTTGTCGTGAAGCCACTCTG-3’	Membrane receptor for SHH and SMO. SHH-PTCH1 releases SMO and induces SMO activity: No
SmoF 5’-CCGCACTAACCTAATGGA-3’ SmoR 5’-AATCGCTGTATTCAACTTGTT-3’	Downstream effector of SHH signaling: No
Gli1F 5’-CTGGTCCACCAACCAACTATGG-3’ Gli1R 5’-CTTGTCCATAATGCTCAAGTCG-3’	Downstream effector of SHH signaling: No
Gli2F 5’-GCCAAGCCATGGTCACATCA-3’ Gli2R 5’-CTGTGTCCTGAGATGGCTGA-3’	Downstream effector of SHH signaling: No
Gli3F 5’-CTCACCTGATTGGGATGTGTCT-3’ Gli3R 5’-TGGAAGACAGTTCCTCCCCTA-3’	Downstream effector of SHH signaling: No
FGF signaling pathway	Protein function: the existence of reports of MAC*[1] phenotypes in the mutants (reference number).
Fgf1F 5’-ACAGGAGCGACCAGCACATTC-3’ Fgf1R 5’-TTCCTCATTTGGTGTCTGCGAG-3’	Secreted signaling molecule in the FGF family protein: No
Fgf2F 5’-GAAGAGCGACCCACACGTCAAA-3’ Fgf2R 5’-CAAGGTACCGGTTGGCACACA-3’	Secreted signaling molecule in the FGF family protein: No
Fgf4F 5’-TGGGCCTCAAAAGGCTTCG-3’ Fgf4R 5’-CGTCGGTAAAGAAAGGCACAC-3’	Secreted signaling molecule in the FGF family protein: No
Fgf7F 5’-GGGCACTATATCTCTAGCTTGC-3’ Fgf7R 5’-GGGTGCGACAGAACAGTCT-3’	Secreted signaling molecule in the FGF family protein: No
Fgf8F 5’-AGAAGACGGAGACCCCTTCGC-3’ Fgf8R 5’-CTTGCCTTTGCCGTTGCTCTTG-3’	Secreted signaling molecule in the FGF family protein: No
Fgfr1F 5’-GCCGTGAAGATGTTGAAGTCC-3’ Fgfr1R 5’-CAATGACATAAAGAGGACCATCC-3’	Membrane receptor for FGFs ligands: No
Fgfr3F 5’-TCGTGGCTGGAGCTACTTC-3’ Fgfr3R 5’-CTCCTGCTGGCTAGGTTCAG-3’	Membrane receptor for FGFs ligands: No

Other genes control ocular morphogenesis	Protein function: the existence of reports of MAC*[1] phenotypes in the mutants (reference number).
Cyp1b1F 5’-ACATCCCCAAGAATACGGTC-3’ Cyp1b1R 5’-TAGACAGTTCCTCACCGATG-3’	Cytochrome P450 subfamily. The mutation cause anterior segment dysgenesis and glaucoma: Yes (S8-S10)
Foxc1F 5’-TTCCACTCGGTGCGGGAAATG-3’ Foxc1R 5’-ACGTGCGGTACAGAGACTGACTG-3’	Forkhead transcription factor. The mutation cause anterior segment dysgenesis: No
Foxc2F 5’-TCCCAGGTGAGCAATGCGAG-3’ Foxc2R5’-TTTGGTGCAGTCGTAAGTGTAGGG-3’	Forkhead transcription factor. The mutation cause anterior segment dysgenesis including iris hypoplasia and severe eccentric pupil: No
Foxe3F 5’-GTCTAACGCTGGCAGCCATCTAC-3’ Foxe3R 5’-CACCTTGACGAAACAGTCGTTGAG-3’	Forkhead transcription factor: Yes (S2)
MipF 5’-AACCTAGCGCTCAACACGCTG-3’ MipR 5’-CCCCGCACCAGTGTAATACATCC-3’	Major ocular lens fiber membrane protein. The mutation causes autosomal dominant cataract: No
MitfF 5’-ATCCCCAAGTCAAATGATCCAGAC-3’ MitfR 5’-TGCATCTCCAGCTCCTGTACTG-3’	Basic helix-loop-helix-leucine zipper transcription factor: Yes (S11)
Nr2e3F 5’-CAGCCAGCCTGTGAGGTT-3’ Nr2e3R 5’-AGAAGCTCAATGCGCTCAG-3’	Retinal nuclear transcription factor. The mutation causes retinal folding, dysplasia and degeneration: No
NrlF 5’-TTCTGGTTCTGACAGTGACTACG-3’ NrlR 5’-TGGGACTGAGCAGAGAGAGG-3’	Basic motif-leucine zipper transcription factor. The mutation causes retinitis pigmentosa: No
Otx2F 5’-GACTGCAGGGCAGAGACG-3’ Otx2R 5’-GGTAGATTTGGAGTGACGGAAC-3’	Homeobox transcription factor: Yes (S3)
Pax6F 5’-AGTTCTTCGCAACCTGGCTA-3’ Pax6R 5’-GTGTTCTCTCCCCCTCCTTC-3’	Paired box transcription factor: Yes (S3)
Pitx2F 5’-AGCTGTGCAAGAATGGCTTT-3’ Pitx2R 5’-CACCATGCTGGACGACATAC-3’	Paired-like homeodomain transcription factor: Yes (S12,S13)
Pitx3F 5’-CTGCTGCGGGACGCACTAGAC-3’ Pitx3R 5’-CCGAGGCCTTCTCCGAGTCAC-3’	Paired-like homeodomain transcription factor: Yes (S14) In addition, aphakia (S15,S16)
Prox1F 5’-CTGGGCCAATTATCACCAGT-3’ Prox1R 5’-GCCATCTTCAAAAGCTCGTC-3’	Homeodomain transcription factor. Prox1 is need for lens fiber differentiation: No
RaxF 5’-CGACGTTCACCACTTACCAA-3’ RaxR 5’-TCGGTTCTGGAACCATACCT-3’	Homeodomain transcription factor: Yes (S3)
Six3F 5’-GGCACTTCGATCCTCTCG-3’ Six3R 5’-GGGCAATTGGGTTTGTTTC-3’	Homeodomain transcription factor. The mutation causes holoprosencephaly: Yes (S3)
Six6F 5’-GCTGCAGCCAAAAACAGACT-3’ Six6R 5’-CGCCTTGCTCGACAGACT-3’	Homeodomain transcription factor. The mutation causes retinal hypoplasia: No

Other genes control ocular morphogenesis	Protein function: the existence of reports of MAC*[1] phenotypes in the mutants (reference number)
Sox2F 5'-TACAGCATGATGCAGGACCA-3' Sox2R 5'-CGAGCTGGTCATGGAGTTGTA-3'	Transcription factor: Yes (S3)
Tmx3F 5'-TTCAGAGACCACTTCCATAGAG-3' Tmx3R 5'-ATTGTTGGGACTGTTAATTCGTC-3'	Protein-disulfide isomerase: Yes (S18)
Vsx2F 5'-CGTAAGAAGCGGCGACAC-3' Vsx2R 5'-TCTGGGTAGTGGGCTTCATT-3'	Homeodomain transcription factor: Yes (S3)
Yap1F 5'-GACTCCGAATGCAGTGTCTT-3' Yap1R 5'-ATCGGAACTATTGGTTGTCA-3'	Hipp pathway effector: Yes (S3)

References (S1-S18) are described in Supplementary References. *[1]microphthalmia, anophthalmia, and coloboma.

Supplementary Table S2 | Incidence of mice with microphthalmia and coloboma at E14.5, E16.5, E18.5 and P0.

	microphthalmia	coloboma	microphthalmia with coloboma
Mice with microphthalmia judged by gross examination			
E14.5			
wild-type	1 (1 right) / 37 (2.7%)	1 (1 right) / 37	1 (1 right) / 37
Lrp4$^{+/-}$	0 / 63 (0%)	1 (1 right) / 63	0 / 63
Lrp4$^{-/-}$	3 (3 right) / 34 (8.8%)	2 (2 right) / 34	1 (1 right) / 34
E16.5			
wild-type	0 / 37 (0%)	0 / 37	0 / 37
Lrp4$^{+/-}$	1 (1 right) / 61 (1.6%)	2 (1 left; 1 right) / 61	1 (1 right) / 61
Lrp4$^{-/-}$	3 (1 left; 2 right) / 32 (9.4%)	2 (2 right) / 32	2 (2 right) / 32
E18.5			
wild-type	2 (2 right) / 177 (1.1%)	1 (1 right) / 177	1 (1 right) /177
Lrp4$^{+/-}$	4 (1 left; 3 right) / 311 (1.3%)	1 (1 right) / 311	1 (1 right) /311
Lrp4$^{-/-}$	16 (3 left; 11 right; 2 both*[1]) / 166 (9.0%)	7 (2 left; 5 right) / 166	5 (1 left; 4 right) / 166
P0			
wild-type	2 (1 right; 1 both*[2]) / 127 (1.6%)	0 / 127	0 / 127
Lrp4$^{+/-}$	2 (1 left; 1 right) / 237 (0.8%)	1 (1 right) / 237	1 (1 right) / 237
Lrp4$^{-/-}$	6 (1 left; 5 right) / 72 (8.3%)	3 (1 left; 2 right) / 72	3 (1 left; 2 right) / 72
E14.5+E16.5+E18.5+P0			
wild-type	5 (4 right; 1 both*[2]) / 378 (1.3%)	2 (2 right) / 378	2 (2 right) / 378
Lrp4$^{+/-}$	7 (2 left; 5 right) / 672 (1.0%)	5 (5 right) / 672	2 (2 right) / 672
Lrp4$^{-/-}$	28 (5 left; 21 right; 2 both*[1]) / 304 (9.2%)	14 (3 left; 11 right) / 304	11 (2 left; 9 right) / 304

Mice with microphthalmia defined as an eyeball with a at least two SDs below the mean of left/right diameter

E14.5	(mean ± SD mm)	total means – 2×SD = 0.94 mm		
wild-type	(1.11±0.07)	0 / 12 (0%)	0 / 12	0 / 12
Lrp4$^{+/-}$	(1.10 ± 0.08)	1 (1 right) / 21 (4.8%)	1 (1 right) / 21	1 (1 right) / 21
Lrp4$^{-/-}$	(1.08 ± 0.10)	1 (1 right) / 10 (10%)	2 (2 right) / 10	1 (1 right) / 10

E16.5	(mean ± SD mm)	total means – 2×SD = 1.14 mm		
wild-type	(1.35 ± 0.10)	1 (1 right) / 26 (3.8%)	1 (1 right) / 26	0 / 26
Lrp4$^{+/-}$	(1.34 ± 0.09)	1 (1 right) / 49 (2.0%)	1 (1 right) / 49	1 (1 right) / 49
Lrp4$^{-/-}$	(1.31 ± 0.12)	5 (1 left ;4 right) / 24 (20.8%)	3 (1 left ; 2 right) /24	3 (1 left ; 2 right) / 24

E18.5	(mean ± SD mm)	total means – 2×SD = 1.42 mm		
wild-type	(1.73 ± 0.15)	1 (1 right) / 70	0 / 70	0 / 70
Lrp4$^{+/-}$	(1.71 ± 0.15)	2 (1 left; 1 right) / 128	2 (1 left; 1 right) / 128	1 (1 right) / 128
Lrp4$^{-/-}$	(1.67 ± 0.18)*[3]	7 (1 left; 5 right; 1 both*[1]) / 65	5 (5 right) / 65	4 (4 right) / 65

P0	(mean ± SD mm)	total means – 2×SD = 1.67 mm		
wild-type	(1.92 ± 0.13)	1 (1 right) / 79	1 (1 right) / 79	1 (1 right) / 79
Lrp4$^{+/-}$	(1.91 ± 0.11)	1 (1 both) / 159	1 (1 both) / 159	1 (1 both) / 159
Lrp4$^{-/-}$	(1.88 ± 0.12)*[3]	7 (2 left; 4 right;1 both*[1]) / 75	4 (1 left; 3 right) / 75	4 (1 left; 3 right) / 75

E14.5+E16.5+E18.5+P0			
wild-type	3 (3 right) / 187 (1.6%)	2 (2 right) / 187	1 (1 right) / 187
Lrp4$^{+/-}$	5 (1 left; 3 right; 1 both) / 357 (1.4%)	5 (1 left; 3 right; 1 both) / 357	4 (3 right; 1 both) / 357
Lrp4$^{-/-}$	20 (4 left; 14 right; 2 both*[1]) / 174 (11.5%)	14 (2 left; 12 right) / 174	12 (2 left; 10 right) /174

*[1]Right eye with coloboma.

*[2]Otocephaly with microphthalmia on both eyes.

*[3]Excluded a very small eye with a little abnormal retinal tissue from calculations.

Supplementary References

S1. C. Liu, S.A. Widen, K.A. Williamson, et al., A secreted WNT-ligand-binding domain of FZD5 generated by a frameshift mutation causes autosomal dominant coloboma, Hum. Mol. Genet. 25 (2016) 1382-1391.

S2. A. Alldredge, S. Fuhrmann, Loss of Axin2 Causes Ocular Defects During Mouse Eye Development Invest. Ophthalmol. Vis. Sci. 57 (2016) 5253-5262.

S3. K.A. Williamson, D.R. FitzPatrick, The genetic architecture of microphthalmia, anophthalmia and coloboma, Eur. J. Med. Genet. 57 (2014) 369-380.

S4. Y. Liu, K. Kawai, S. Khashabi, et al., Inactivation of Smad4 leads to impaired ocular development and cataract formation, Biochem. Biophys. Res. Commun. 400 (2010) 476-482.

S5. J. Li, S. Wang, C. Anderson, et al., Requirement of Smad4 from ocular surface ectoderm for retinal development, PLoS One 11 (2016) e0159639.

S6. L.A. Schimmenti, J. de la Cruz, R.A. Lewis, et al., Novel mutation in Sonic hedgehog in non-syndromic colobomatous microphthalmia, Am. J. Med. Genet. 116A (2003) 215-221.

S7. P. Bakrania, S.A. Ugur Iseri, A.W. Wyatt, et al., Sonic hedgehog mutations are an uncommon cause of developmental eye anomalies, Am. J. Med. Genet. 152A (2010) 1310-1313.

S8. L.M. Reis, R.C. Tyler, R. Zori, et al., A case of 22q11.2 deletion syndrome with Peters anomaly, congenital glaucoma, and heterozygous mutation in CYP1B1, Ophthalmic Genet. 36 (2015) 92-94.

S9. I. Prokudin, C. Simons, J.R. Grigg, et al., Exome sequencing in developmental eye disease leads to identification of causal variants in GJA8, CRYGC, PAX6 and CYP1B1, Eur. J. Hum. Genet. 22 (2014) 907-915.

S10. L.M. Reis, R.C. Tyler, E. Weh, et al., Analysis of *CYP1B1* in pediatric and adult glaucoma and other ocular phenotypes, Mol. Vis. 22 (2016) 1229-1238.

S11. E. Steingrimsson., K.J. Moore, M.L. Lamoreux, et al., Molecular basis of mouse microphthalmia (mi) mutations helps explain their developmental and phenotypic consequences. Nature Genet. 8 (1994) 256-263.

S12. A.L. Evans, P.J. Gage, Expression of the homeobox gene Pitx2 in neural crest is required for optic stalk and ocular anterior segment development, Hum. Molec. Genet. 14 (2005) 3347-3359.

S13. P.J. Gage, H. Suh, S.A. Camper, Dosage requirement of Pitx2 for development of multiple organs, Development 126 (1999) 4643-4651.

S14. D. Becker, J. Tetens, A. Brunner, et al., Microphthalmia in Texel sheep is associated with a missense mutation in the paired-like homeodomain 3 (PITX3) gene, PLoS One 5 (2010) e8689.

S15. K. Wada, Y. Matsushima, T. Tada, et al., Expression of truncated PITX3 in the developing lens leads to microphthalmia and aphakia in mice, PLoS One 9 (2014) e111432.

S16. E.V. Semina, J.C. Murray, R. Reiter, et al., Deletion in the promoter region and altered expression of Pitx3 homeobox gene in aphakia mice, Hum. Mol. Genet. 9 (2000) 1575-1585.

S17. D.E. Wallis, E. Roessle, U. Hehr, et al., Mutations in the homeodomain of the human SIX3 gene cause holoprosencephaly, Nat. Genet. 22 (1999) 196-198.
S18. R. Chao, L. Nevin, P. Agarwal, et al., A Male with Unilateral Microphthalmia Reveals a Role for TMX3 in Eye Development, PLoS ONE 5 (2010) e10565.